The HKU Scholars Hub   The University of Hong Kong   香港大學學術庫

Title	Diffusion tensor imaging of somatosensory tract in cervical spondylotic myelopathy and its link with electrophysiological evaluation
Author(s)	Wen, Chunyi; Cui, Jiaolong; Mak, Kincheung; Luk, Keith D K; Hu, Yong
Citation	The Spine Journal, 2014, v. 14, n. 8, p. 1493-1500
Issued Date	2014
URL	http://hdl.handle.net/10722/205814
Rights	NOTICE: this is the author's version of a work that was accepted for publication in Spine Journal. Changes resulting from the publishing process, such as peer review, editing, corrections, structural formatting, and other quality control mechanisms may not be reflected in this document. Changes may have been made to this work since it was submitted for publication. A definitive version was subsequently published in Spine Journal, 2014, v. 14, n. 8, p. 1493-1500. DOI: 10.1016/j.spinee.2013.08.052

1   **Title**:   Diffusion Tensor Imaging of Somatosensory Tract in Cervical Spondylotic

2   Myelopathy and Its Link with Electrophysiological Evaluation

3   **Running Title**: DTI in CSM

4

5   Chun-Yi Wen [#], Jiao-Long Cui [#], Kin-Cheung Mak, Keith Dip-Kei. Luk, and Yong Hu [*]

6   Department of Orthopaedics and Traumatology, Li Ka Shing Faculty of Medicine, The

7   University of Hong Kong

8   "[#]" Equally contribution to this manuscript

9   "[*]" Corresponding Author

10   Dr Yong Hu

11   Dept. of Orthopaedics and Traumatology,

12   The University of Hong Kong

13   Address: 12 Sandy Bay Road, Pokfulam, Hong Kong

14   Email address: yhud@hku.hk;

15   Tel: (852) 29740359; Fax: (852) 29740335

16

Abstract

Background and Context: Abnormal somatosensory evoked potential (SEP), i.e., prolonged latency, has been associated with poor surgical prognosis of cervical spondylotic myelopathy (CSM).

Purpose: To further characterize the extent of microstructural damage to the somatosensory tract in CSM patients using diffusion tensor imaging (DTI).

Study Design/Setting: Retrospective study.

Patient Sample: A total of 40 volunteers (25 healthy subjects and 15 CSM patients).

Outcome Measures: Clinical, electrophysiological and radiological evaluations were performed using the Japanese Orthopaedic Association (JOA) scoring system, SEP and cord compression ratio in anatomic MR images respectively. Axial diffusion MR images were taken using a pulsed gradient, spin-echo-echo-planar imaging (SE-EPI) sequence with a 3T MR system. The diffusion indices in different regions of the spinal cord were measured.

Methods: Comparison of diffusion indices among healthy and myelopathic spinal cord with intact and impaired SEP responses were performed using one-way ANOVA.

Results: In healthy subjects, FA values were higher in the dorsal (0.73 ± 0.11) and lateral columns (0.72 ± 0.13) than in the ventral column of WM (0.58 ± 0.10), e.g., at C4/5 ($p<0.05$). FA was dramatically dropped in the dorsal (0.54 ± 0.16) and lateral columns (0.51 ± 0.13) with little changes in the ventral column (0.48 ± 0.15) at the compressive lesions in CSM patients. There were no significant differences in the JOA scores or cord compression ratios between CSM patients with or without abnormal SEP. However, patients with abnormal SEP showed a FA decrease in the dorsal column cephalic to the lesion (0.56 ± 0.06), i.e., at C1/2, compared with healthy subjects (0.66 ± 0.02), but the same decrease was not observed for those without a SEP abnormality (0.67 ± 0.02).

Conclusion: Spinal tracts were not uniformly affected in the myelopathic cervical cord. Changes in diffusion indices could delineate focal or extensive myelopathic lesions in CSM,

1   which could account for abnormal SEP. DTI analysis of spinal tracts might provide additional

2   information not available from conventional diagnostic tools for prognosis of CSM.

3   **Key words**: Cervical Spondylotic Myelopathy, Diffusion Tensor Imaging, Spinal Cord,

4   Fractional Anisotropy, Microstructure

1 **Introduction**

2   Cervical spondylotic myelopathy (CSM) is the most common type of spinal cord

3 dysfunction in patients older than 55 years [1-3]. The severity of somatosensory dysfunction,

4 i.e. the prolonged latency of somatosensory evoked potential (SEP), has been identified as an

5 indicator for the poor prognosis in CSM patients after surgical management . However, the

6 information regarding the extent of somatosensory tract damage in CSM patients remains to

7 be explored.

8   The emerging diffusion tensor imaging (DTI) technique provides in vivo detection of the

9 microstructure of the spinal cord parenchyma [5]. Fractional anisotropy (FA) and diffusivities,

10 e.g., mean diffusivity (MD), axial and radial diffusivities (AD and RD), were derived from

11 the diffusion tensor matrix, which are commonly used in DTI analysis to describe the voxels'

12 diffusion properties [6]. Above diffusion indices are attributed to the densely packed axonal

13 membranes in the spinal cord, and they may reflect microarchitectural changes associated

14 with the demyelination process and axon damage in neurological injury and disease [7,8].

15 Feasibility of DTI has been used for CSM patients in previous studies [9-17]. However, little

16 is known about the specific spinal tract damages in CSM due to the poor quality of diffusion

17 MR images in previous studies under relatively lower magnetic field strengths, i.e., 0.2 and

18 1.5 Tesla, or sagittal slicing of the cervical spinal cord [9-17]. Several approaches were

19 employed to improve the quality of diffusion MR images, including use of a 3.0-Tesla MRI

20 scanner, optimizing the axial slice thickness to achieve a good signal/noise ratio (SNR) and

21 reducing motion artifacts through cardiac/respiratory gating [18,19]. The improved image

22 quality, with a clear separation of gray and white matter structures, makes it possible to

23 analyze the microarchitecture of the spinal tracts anatomically.

24   This study aimed to (1) characterize the diffusion properties of the ventral, lateral and

25 dorsal columns in the healthy and myelopathic cervical cord using diffusion MR images and

26 (2) correlate SEP status, i.e., normal or prolonged latency, with DTI findings in CSM patients.

1 **Materials and Methods**

2 *Subjects*

3   The institutional review board of research ethics approved all experimental procedures in

4 this study. A total of forty volunteers were recruited with informed consent (25 healthy

5 subjects at the age of 52±7 years old and 15 CSM patients at the age of 60±9 years old). All

6 volunteers were screened to confirm their eligibility before the study. The inclusion criteria

7 for healthy subjects were with intact sensory and motor function and a negative Hoffman's

8 sign under physical examination. Those having any neurological signs or symptoms or any

9 past history of neurological injury, disease or surgeries were excluded. Experienced spinal

10 surgeons made clinical diagnoses based on the insidious and chronic course, neurological

11 deficit and radiological findings of degenerative intervertebral discs and spondylosis. The

12 CSM patients' neurological deficits were evaluated via physical examination and the

13 modified Japanese Orthopaedic Association (mJOA) score, with the highest score being 17

14 [20,21].

15 *Electrophysiological assessments*

16   The functional integrity of the spinal cord was evaluated using somatosensory evoked

17 potential (SEP) [4]. In brief, stimulation was applied to the median nerve on the wrists, while

18 SEP signals were recorded from the C3 in response to right limb stimulation and from the C4

19 in response to left limb stimulation, with the reference electrode at Fz according to the

20 international 10–20 system [6]. The data were inspected for the presence of the main peaks

21 N19/P22 by an experienced electrophysiologist. The latency and amplitude of SEP signals

22 from CSM patients were compared with previously published healthy criteria (latency:

23 18.40±0.71 ms; amplitude: 1.23±0.50 µV) [4]. The impaired SEP in CSM patients were

24 defined as delayed N19 latency (exceeding 2.5 SD),regardless of the peak-to-peak amplitude

25 (< 0.5 µV), or waveform disappearance [4].

26 *MRI Scanning*

1   All images were taken via a 3.0-Tesla MRI scanner (Philips Achieva). During the

2   acquisition process, the subject was placed in a supine position with the sense neuro-vascular

3   (SNV) head and neck coil enclosing the cervical region and instructed not to swallow to

4   minimize motion artifacts. The subject was then scanned to produce anatomical T1-weighted

5   (T1W) images, T2-weighted (T2W) images and diffusion tensor images (DTI).

6   Sagittal and axial T1W and T2W images were acquired for each subject. A fast spin echo

7   (FSE) sequence was employed. A total of 11 sagittal images covering the whole cervical

8   spinal cord were acquired. Cardiac vectorcardiogram (VCG) triggering was applied to

9   minimize the pulsation artifact from CSF. A total of 12 transverse images covering the

10   cervical spinal cord from C1 to C7, each of which was placed at the center of either a

11   vertebrae or intervertebral disc, were acquired. Diffusion MRI images were acquired using

12   the pulsed sequence of single-shot spin-echo echo-planar imaging (SE-EPI). Diffusion

13   encoding was in 15 non-collinear and non-coplanar diffusion directions with a b-value = 600

14   s/mm^2. The image slice planning was the same as that for the anatomical axial T1W and T2W

15   images, with 12 slices covering the cervical spinal cord from C1 to C7. The duration of

16   diffusion tensor imaging (DTI) averaged 24 minutes per subject with an average heart rate of

17   60 beats per minute. Spatial saturation with Spectral Presaturation with Inversion Recovery

18   (SPIR) was applied to suppress the fold-over effect.

19   *Image analysis*

20   The morphometry of the spinal cord were analyzed using the previously reported

21   methods [22], including measurement of cervical cord compression using the anterior-

22   posterior diameter/transverse diameter ratio in axial T2W images. Intramedullary signal

23   changes were recorded based on both T2W and T1W images.

24   Diffusion measurement was performed using DTIStudio software (Version 2.4.01 2003,

25   Johns Hopkins Medical Institute, Johns Hopkins University). Image volume realignment and

26   3D rigid body registration with different diffusion gradients were conducted using the

1   Automated Image Registration (AIR) program (Laboratory of Neuroimaging, UCLA) to

2   reduce the effect of motion artifacts. The realigned and co-registered diffusion- weighted data

3   were double checked for image quality and then used to estimate diffusion tensors, including

4   three eigenvalues ($\lambda 1$, $\lambda 2$ and $\lambda 3$) and the corresponding eigenvectors. Maps of the fractional

5   anisotropy (FA) and axial and radial diffusivity (AD and RD) were derived from the diffusion

6   matrix accordingly.

7   The regions of interest (ROIs) were defined in different areas of the cervical spinal cord:

8   the ventral, lateral and dorsal columns of white matter (WM) (Figure 1) [23]. The diffusion

9   indices were calculated by averaging all selected voxels in the ROIs using ImageJ (National

10   Institute of Health, USA).

11   *Statistical analysis*

12   The FA, AD and RD values in different regions of the spinal cord were calculated at

13   each vertebrae and disc level along the whole cervical spine (Figure 2). The degenerated disc

14   level(s) and adjacent vertebrae level(s) were defined as the spondylotic myelopathic lesion

15   segment for statistical analysis. Comparisons among healthy and myelopathic spinal cord

16   with intact and impaired SEP responses were performed using one-way ANOVA. The level of

17   significance was set at $p<0.05$. All data analyses were performed using SPSS 15.0 analysis

18   software (SPSS Inc., Chicago, IL, USA).

19

1   **Results**

2   *Clinical, radiological and electrophysiological data*

3   A total of fifteen CSM patients presented with severe neurological deficits as indicated

4   by their significant mJOA scores (CSM: 9.8±1.0, full score 17) and the compression of the

5   cervical cord (0.35±0.07) compared to healthy subjects (0.52±0.05, p<0.001) (Table 1, Figure

6   2).

7   Among fifteen CSM patients, five of them presented prolonged latency in SEP (latency:

8   21.90±1.22 ms; amplitude: 0.87±0.42 μV) and were classified as the CSM_lat+ group. The

9   remaining CSM patients, who presented normal SEP or only decreased amplitude (latency:

10   17.81±1.06 ms; amplitude: 1.14±0.64 μV), were classified as the CSM_lat- group. There were

11   no significant differences in the age of patients (CSM_lat+: 62±8 years, CSM_lat-: 59±10

12   years), duration of disease (CSM_lat+: 6.1±8 years, CSM_lat-: 6.1±2.3 years) or mJOA score

13   (CSM_lat+: 10.0±0.9, CSM_lat-: 9.4±1.1) between these two groups. Intramedullary signal

14   changes in T2 or T1 images appeared more frequently in the CSM_lat+ group (Table 1).

15   *Regional differences in diffusion anisotropy in the healthy cervical spinal cord*

16   The tissue microarchitecture was not uniform in the cervical spinal tracts of healthy

17   subjects. FA values were significantly higher in the dorsal (0.73±0.11) and lateral columns

18   (0.72±0.13) than those in the ventral column of WM (0.58±0.10) (p<0.05), e.g., at C4/5. At

19   the same level, there were no statistically significant differences in AD values between the

20   different regions of white matter (dorsal column: $2.067 \pm 0.197 \times 10^{-3}$; lateral column:

21   $2.081 \pm 0.191 \times 10^{-3}$; ventral column: $2.130 \pm 0.242 \times 10^{-3}$), whereas RD values were relatively

22   lower in the somatosensory tracts (dorsal column: $0.596 \pm 0.243 \times 10^{-3}$; lateral column:

23   $0.612 \pm 2.23 \times 10^{-3}$; ventral column: $0.770 \pm 0.177 \times 10^{-3}$) (Figure 3).

24   *Changes in diffusion anisotropy were region-dependent*

25   The diffusion indices of the myelopathic cord changed in all three columns in the white

26   matter. For example, at the level of C4/5, the AD values were significantly higher in all

8

1   regions of the myelopathic cord (dorsal column: $3.139 \pm 0.447 \times 10^{-3}$; lateral column:

2     $2.857 \pm 0.371 \times 10^{-3}$; ventral column: $3.356 \pm 0.266 \times 10^{-3}$) than those in the healthy cord (dorsal

3   column: $2.067 \pm 0.197 \times 10^{-3}$; lateral column: $2.081 \pm 0.191 \times 10^{-3}$; ventral column:

4     $2.130 \pm 0.242 \times 10^{-3}$; $p < 0.001$). Increased RD values were also detected in the myelopathic cord

5   (dorsal column: $1.500 \pm 0.487 \times 10^{-3}$; lateral column: $1.498 \pm 0.320 \times 10^{-3}$; ventral column:

6     $1.610 \pm 0.080 \times 10^{-3}$) in comparison with the healthy cord (dorsal column: $0.596 \pm 0.210 \times 10^{-3}$;

7   lateral column: $0.612 \pm 0.223 \times 10^{-3}$; ventral column: $0.770 \pm 0.177 \times 10^{-3}$; $p < 0.001$).

8   By contrast, the FA changes in the myelopathic cord were region-dependent. As shown

9   in Figures 1 and 2, a significant change in FA was observed in the dorsal (0.54 ± 0.16) and

10   lateral columns (0.51 ± 0.13) of the myelopathic spinal cord under anterior compression; while

11   the ventral column of myelopathic spinal cord were relatively spared (0.48 ± 0.15). The

12   regional differences in FA, observed in healthy spinal cord, were absent in the myelopathic

13   cord.

14   *Diffusion anisotropy drop cephalic to the lesion*

15   As compared to healthy subjects, CSM patients with intact SEP (normal latency) showed

16   the decrease of FA localized at the dorsal and lateral columns of white matter in myelopathic

17   spinal cords. By contrast, the decrease of FA was much more extensive in patients with

18   impaired SEP (prolonged latency), involving three columns of white matter (dorsal column:

19   0.57 ± 0.05; lateral column: 0.58 ± 0.03; ventral column: 0.48 ± 0.03) (Figure 4). In addition, it

20   not only occurred at the compressive lesion, but also at the cephalic level to the lesion in all

21   three columns of white matter (dorsal column: 0.57 ± 0.06; lateral column: 0.57 ± 0.04; ventral

22   column: 0.53 ± 0.02) (Figures 4, 5).

1 **Discussion**

2   DTI was employed to evaluate regional deficits in the myelopathic spinal cord. It was

3 found that the spinal tracts were not uniformly affected in CSM. The CSM-related changes of

4 diffusion anisotropy were region-dependent, afflicting the dorsal and lateral columns and

5 relatively sparing the ventral column. It was in a good agreement with histopathological

6 findings under clinical autopsy examination [1].

7   In consistence with previous DTI studies of CSM[11-19], the present study

8 demonstrated FA decrease and apparent diffusion coefficient (ADC) or mean diffusivity

9 increase in CSMThe diffusivity changes in CSM reflect the increase in the strength of water

10 molecule movement in the enclosed spinal cord when passing through a narrow canal. This

11 increase may be part of the spinal cord's initial adaptation under chronic compression in a

12 progressive stenotic canal. The unconstrained water molecules in the myelopathic cord

13 present the decrease of diffusion anisotropy under DTI examination.

14   AD and RD of the myelopathic cord were elevated in all three columns, and they did not

15 show the same regional differences as those observed for FA. By contrast, FA pattern of the

16 myelopathic cord was more compatible with histopathological features of previously

17 published clinical autopsy studies [4,5]. FA appeared to reflect demyelination and axon

18 damage more appropriately in CSM cases in comparison with AD and RD, although they

19 were once used to detect microstructural changes in other spinal cord disorders, e.g., multiple

20 sclerosis [9,10].

21

22   Clinically, the prolonged latency of SEP has been reported as an indicator for the poor

23 prognosis of CSM after surgeries [4]. It was also found in a rat model that the normal or

24 prolonged latency of SEP were in a good association with the severity of microstructural

25 damages in the chronic compressive spinal cord [37]. In this study, diffusion MR imaging of

26 spinal tracts unveiled that a decrease of FA at the cephalic level of myelopathic cord to the

1   compressive lesion indicated anterograde degeneration of somatosensory spinal tract, so-

2   called Wallerian degeneration. This finding specifically provided the structural basis of

3   prolonged latency of SEP in myelopathic human spinal cord. The JOA assessment is a global

4   assessment for myelopathic severity [28].However, spinal tracts are not uniformly affected in

5   CSM, which cannot be reflected by a global assessment such as the JOA score. We did not

6   find a difference in the sums of the JOA scores between CSM patients with or without

7   prolonged latency. The value of the JOA score system in predicting surgical outcomes for

8   CSM patients remains controversial [29]. As such, the regional analysis of diffusion MR

9   images of the myelopathic cord might provide additional information to the current

10   assessments, including the JOA score system, anatomic MR images and SEP, to formulate a

11   comprehensive evaluation approach for clinical diagnosis and prognosis of CSM.

12   The severity of cord compression did not necessarily correlate with the signs and

13   symptoms of CSM patients [30-32]. For example, there were cases with significant cord

14   compression but without any neurological signs, or with mild cord compression but with

15   development of neurological signs [33,34]. We found that there was no significant difference

16   in the compression ratio of the myelopathic cord with or without prolonged latency in SEP,

17   although there was a difference in the extent of cord damage between the two groups.

18   The clinical significance of T2 hyperintensity [29,35-38], and T1 hypointensity [39,40]

19   was also documented in CSM patients. It was found that signal changes of the myelopathic

20   cord were commonly present in CSM patients with prolonged latency of SEP. However, such

21   signal changes in the cervical cord are non-specific, which covers a wide spectrum of

22   pathological changes such as edema and hemorrhage (T2 hyperintensity) or cyst (T1

23   hypointensity). In contrast, DTI might provide more specific information on demyelination

24   and axon damage in spinal tracts of the myelopathic cord.

25   In summary, DTI could provide a more sensitive and specific measurement for spinal

26   tract damage in CSM than the conventional clinical, electrophysiological and radiological

1   assessments. Limited to a cross-sectional observation on a small number of CSM patients, the

2   exact diagnostic and prognostic values of DTI in CSM needs to be verified in a large-scale,

3   prospective study in the near future.

4

1   References

2   1.   McCormick WE, Steinmetz MP, Benzel EC. Cervical spondylotic myelopathy: make the difficult

3   diagnosis, then refer for surgery. Cleve Clin J Med. 2003;70(10):899-904.

4   2.   Ichihara K, Taguchi T, Sakuramoto I, Kawano S, Kawai S. Mechanism of the spinal cord injury

5   and the cervical spondylotic myelopathy: new approach based on the mechanical features of the spinal

6   cord white and gray matter. J Neurosurg. 2003;99(3 Suppl):278-85.

7   3.   Rao R. Neck Pain, Cervical Radiculopathy, and Cervical Myelopathy: Pathophysiology, Natural

8   History, and Clinical Evaluation. The Journal of Bone & Joint Surgery. 2002;84(10):1872-81.

9   4.   Hu Y, Ding Y, Ruan D, Wong YW, Cheung KM, Luk KD. Prognostic value of somatosensory-

10   evoked potentials in the surgical management of cervical spondylotic myelopathy. Spine.

11   2008;33(10):E305-10.

12   5.   Thurnher MM, Law M. Diffusion-weighted imaging, diffusion-tensor imaging, and fiber

13   tractography of the spinal cord. Magn Reson Imaging Clin N Am. 2009;17(2):225-44.

14   6.   Basser PJ, Jones DK. Diffusion-tensor MRI: theory, experimental design and data analysis - a

15   technical review. NMR in Biomedicine. 2002;15:456-67.

16   7.   DeBoy CA, Zhang J, Dike S, et al. High resolution diffusion tensor imaging of axonal damage in

17   focal inflammatory and demyelinating lesions in rat spinal cord. Brain. 2007;130:2199-210.

18   8.   Giorgio A, Palace J, Johansen-Berg H, et al. Relationships of brain white matter microstructure

19   with clinical and MR measures in relapsing-remitting multiple sclerosis. J Magn Reson Imaging.

20   2010;31(2):309-16.

21   9.   Budzik JF, Balbi V, Le Thuc V, Duhamel A, Assaker R, Cotten A. Diffusion tensor imaging and

22   fibre tracking in cervical spondylotic myelopathy. European radiology. 2011;21(2):426-33.

23   10.   Demir A, Ries M, Moonen CT, et al. Diffusion-weighted MR imaging with apparent diffusion

24   coefficient and apparent diffusion tensor maps in cervical spondylotic myelopathy. Radiology.

25   2003;229(1):37-43.

26   11.   Kara B, Celik A, Karadereler S, et al. The role of DTI in early detection of cervical spondylotic

27   myelopathy: a preliminary study with 3-T MRI. Neuroradiology. 2011.

28   12.   Kerkovsky M, Bednarik JAP, Dusek L, et al. Magnetic Resonance Diffusion Tensor Imaging in

29   Patients With Cervical Spondylotic Spinal Cord Compression: Correlations Between Clinical and

30   Electrophysiological Findings. Spine (Phila Pa 1976). 2011.

31   13.   Voss HU, Hartl R, Jr FWG, Heier LA, Ballon DJ, Ulug AM. Diffusion Tensor Imaging in Cervical

32   Spondylotic Myelopathy. World Spine Journal. 2007;2(3):140-7.

33   14.   Song T, Chen WJ, Yang B, et al. Diffusion tensor imaging in the cervical spinal cord. Eur Spine J.

34   2011;20(3):422-8.

35   15.   Xiangshui M, Xiangjun C, Xiaoming Z, et al. 3 T magnetic resonance diffusion tensor imaging

36   and fibre tracking in cervical myelopathy. Clin Radiol. 2010;65(6):465-73.

37   16.   Mamata H, Jolesz FA, Maier SE. Apparent diffusion coefficient and fractional anisotropy in spinal

38   cord: age and cervical spondylosis-related changes. J Magn Reson Imaging. 2005;22(1):38-43.

39   17.   Facon D, Ozanne A, Fillard P, Lepeintre J-F, Tournoux-Facon C, Ducreux D. MR Diffusion Tensor

1   Imaging and Fiber Tracking in Spinal Cord Compression. Am J Neuroradiol. 2005;26:1587-94.

2   18.   Ng MC, Ho JT, Ho SL, et al. Abnormal diffusion tensor in nonsymptomatic familial amyotrophic

3   lateral sclerosis with a causative superoxide dismutase 1 mutation. J Magn Reson Imaging. 2008;27(1):8-

4   13.

5   19.   Cui JL, Wen CY, Hu Y, Li TH, Luk KD. Entropy-based analysis for diffusion anisotropy mapping

6   of healthy and myelopathic spinal cord. Neuroimage. 2010.

7   20.   Yonenobu K, Abumi K, Nagata K, Taketomi E, Ueyama K. Interobserver and intraobserver

8   reliability of the japanese orthopaedic association scoring system for evaluation of cervical compression

9   myelopathy. Spine (Phila Pa 1976). 2001;26(17):1890-4; discussion 5.

10   21.   Ono K, Ebara S, Fuji T, Yonenobu K, Fujiwara K, Yamashita K. Myelopathy hand. New clinical

11   signs of cervical cord damage. The Journal of bone and joint surgery British volume. 1987;69(2):215-9.

12   22.   Fujiwara K, Yonenobu K, Hiroshima K, Ebara S, Yamashita K, Ono K. Morphometry of the

13   cervical spinal cord and its relation to pathology in cases with compression myelopathy. Spine (Phila Pa

14   1976). 1988;13(11):1212-6.

15   23.   Hesseltine SM, Law M, Babb J, et al. Diffusion tensor imaging in multiple sclerosis: assessment

16   of regional differences in the axial plane within normal-appearing cervical spinal cord. AJNR Am J

17   Neuroradiol. 2006;27(6):1189-93.

18   24.   Matsumoto M, Toyama Y, Ishikawa M, Chiba K, Suzuki N, Fujimura Y. Increased signal intensity

19   of the spinal cord on magnetic resonance images in cervical compressive myelopathy. Does it predict the

20   outcome of conservative treatment? Spine (Phila Pa 1976). 2000;25(6):677-82.

21   25.   Bednarik J, Kadanka Z, Dusek L, et al. Presymptomatic spondylotic cervical myelopathy: an

22   update predictive model. Eur Spine J. 2008;17:421-31.

23   26.   Kadanka Z, Kerkovshy M, Bednarik J, Jarkovshy J. Cross-sectional Transverse Area and

24   Hyperintensities on Magnetic Resonance Imaging in Relation to the Clinical Picture in Cervical

25   Spondylotic Myelopathy. Spine. 2007;32(23):2573-7.

26   27.   Baptiste DC, Fehlings MG. Pathophysiology of cervical myelopathy. The Spine Journal.

27   2006;6:190S-7S.

28   28.   Baron EM, Young WF. Cervical Spondylotic Myelopathy: A Brief Review of its Pathophysiology,

29   Clinical Course, and Diagnosis. Neurosurgery. 2007;60.

30   29.   Kohno K, Kumon Y, Oka Y, Matsui S, Ohue S, Sakaki S. Evaluation of prognostic factors

31   following expansive laminoplasty for cervical spinal stenotic myelopathy. Surgical neurology.

32   1997;48(3):237-45.

33   30.   Ohshio I, Hatayama A, Kaneda K, Takahara M, Nagashima K. Correlation between

34   histopathologic features and magnetic resonance images of spinal cord lesions. Spine. 1993;18(9):1140-9.

35   31.   Wada E, Ohmura M, Yonenobu K. Intramedullary changes of the spinal cord in cervical

36   spondylotic myelopathy. Spine. 1995;20(20):2226-32.

37   32.   Yone K, Sakou T, Yanase M, Ijiri K. Preoperative and postoperative magnetic resonance image

38   evaluations of the spinal cord in cervical myelopathy. Spine. 1992;17(10 Suppl):S388-92.

39   33.   Mastronardi L, Elsawaf A, Roperto R, et al. Prognostic relevance of the postoperative evolution of

1   intramedullary spinal cord changes in signal intensity on magnetic resonance imaging after anterior

2   decompression for cervical spondylotic myelopathy. Journal of neurosurgery Spine. 2007;7(6):615-22.

3   34.   Vedantam A, Jonathan A, Rajshekhar V. Association of magnetic resonance imaging signal

4   changes and outcome prediction after surgery for cervical spondylotic myelopathy. Journal of neurosurgery

5   Spine. 2011;15(6):660-6.

6   35.   Mummaneni PV, Kaiser MG, Matz PG, et al. Preoperative patient selection with magnetic

7   resonance imaging, computed tomography, and electroencephalography: does the test predict outcome after

8   cervical surgery? Journal of neurosurgery Spine. 2009;11(2):119-29.

9   36.   Ichihara K, Taguchi T, Shimada Y, Sakuramoto I, Kawano S, Kawai S. Gray matter of the bovine

10   cervical spinal cord is mechanically more rigid and fragile than the white matter. J Neurotrauma.

11   2001;18(3):361-7.

12   37.   Hu Y, Wen CY, Li TH, Cheung MM, Wu EX, Luk KD. Somatosensory-evoked potentials as an

13   indicator for the extent of ultrastructural damage of the spinal cord after chronic compressive injuries in a

14   rat model. Clinical neurophysiology : official journal of the International Federation of Clinical

15   Neurophysiology. 2011;122(7):1440-7.

16   38.   Cheung WY, Arvinte D, Wong YW, Luk KD, Cheung KM. Neurological recovery after surgical

17   decompression in patients with cervical spondylotic myelopathy - a prospective study. International

18   orthopaedics. 2008;32(2):273-8.

19

20

Figure Legends

Figure 1. The representative anatomic (A, F), diffusion MR images (B, C, G, H) and fiber tractography (D, E, I, J) of healthy (A~E) and myelopathic spinal cord (F~G). The regions of interest are defined based on the anatomy of the spinal cord in axial slices of the fractional anisotropy (FA) mapping (C, F). The gray matter ("*") is defined as the central portion of the spinal cord with low gray scale on the FA map; then the ventral, lateral and dorsal columns of white matter are defined accordingly (C. H). Compared with the healthy cord, the tracking of water molecules movement significantly changes in the dorsal and lateral aspects of the myelopathic cord (I, J: white arrow).

Figure 2. The characterization of diffusion properties of healthy (left column) and the myelopathic spinal cord (right column) in the ventral, lateral and dorsal columns of white matter by anatomic levels along the length of the cervical spine. FA values significantly drop in the dorsal and lateral columns with relative sparing in the ventral column (shown in the upper row). Yet the AD and RD values are increased in all three columns of white matter (shown in the middle and lower rows). Abbreviations: FA: fractional anisotropy; AD: axial diffusivity; RD: radial diffusivity.

Figure 3. Gross morphometry of the spinal cord was evaluated via measurement of the compression ratio (anterior-posterior distance divided by transverse distance of the spinal cord). Generally, the compression ratio decreases in the myelopathic spinal cord. There is no statistically significant difference in the compression ratio between the myelopathic cord with (CSM_lat+) or without prolonged latency (CSM_lat-). ("*" Indicates statistical significance at $p<0.05$ with one-way ANOVA and *post-hoc* test).

Figure 4. The representative anatomic (A, E, I), diffusion MR images (B, F, J) and fiber tractography (C, D, G, H, K and M) of healthy (A~D) and the myelopathic spinal cord with (I~M) or without prolonged latency (E~H) at C1/2 level cephalic to myelopathic lesions. The myelopathic cord with prolonged latency demonstrate significantly lower FA mapping (J) and disturbance of fiber tracking (K, M) at the upper cervical region cephalic to the chronic compressive lesions compared with those without prolonged latency, as well as the healthy cord.

Figure 5. A comparison of the diffusion anisotropy of the dorsal (A), lateral (B) and ventral columns (C) of white matter among healthy and the myelopathic spinal cord with (CSM_lat+) or without prolonged latency (CSM_lat-). In the CSM_lat- group, FA drops mainly in the dorsal and lateral columns. Yet in the CSM_lat+ group, the changes in FA are much more extensive not only at the lesion level but cephalic to the lesion, and involved in all three columns ("*" Indicates statistical significance at $p<0.05$ with one-way ANOVA and *post-hoc* test).

Table 1 Summary of clinical and radiological data of the patients of cervical spondylotic myelopathy

Case	Gender/age	From symptom onset to imaging	JOA score	Hoffman Sign	Finger Escape Sign	Babinski Sign	Ankle Clonus	Romberg Test	Spinal canal	Spinal cord		Stenostic level(s)	SEP	
										T1W	T2W		Latency	Amplitude
1	F/44	3 years	10.0	-	1	+	-	+	PID	-	-	C5~6	-	+
2	F/46	5 years	11.5	+	2	+	-	+	PID	-	-	C4~5, C5~6	-	+
3	M/54	5 years	9.5	-	0	+	-	+	PID, spondylosis	-	Focal hyperintense signals	C5~6	-	+
4	F/61	4 years	11.0	+	1	-	-	-	PID	-	-	C4~5, C5~6	-	-
5	M/57	8 years	8.5	+	1	-	-	-	PID	-	-	C3~4	-	-
6	F/58	4.5 years	10.0	-	1	+	-	+	PID, spondylosis	-	Focal hyperintense signals	C3~4, C4~5, C5~6	-	+
7	M/61	8 years	9.5	+	1	+	-	+	PID	-	-	C3~4	-	-
8	F/68	7 years	10.0	-	4	+	-	+	PID	-	-	C4~5	-	-
9	M/71	>10 years	11.0	+	2	+	+	+	PID	-	-	C3~4, C4~5, C5~6	-	+
10	M/72	10 years	9.0	+	0	+	-	-	PID	-	-	C4~5, C5~6	-	-
11	F/54	6 years	10.0	+	3	+	+	N.T.	PID, spondylosis	Multi-segmental hypointense signals	Multi-segmental hyperintense signals	C3~4, C4~5, C5~6	+	+
12	F/58	3 years	8.5	+	1	+	-	+	PID	-	-	C4~5, C5~6	+	+
13	M/65	5 years	11.0	+	3	+	+	N.T.	PID, spondylosis	-	Focal hyperintense signals	C4~5, C5~6	+	-
14	M/66	7 years	9.0	+	2	+	+	+	PID	-	Focal hyperintense signals	C5~6	+	+
15	F/74	10 years	8.5	+	4	+	+	N.T.	PID	-	-	C3~4	+	+

Abbreviations: SEP: Somatosensory evoked potentials; PID: protrusion of intervertebral disc;

Note: "+"/"-" indicates the presence (or absence) of pathological signs. Finger escape signs were graded as: "0" all, none deficiency; "1" little finger unable to hold adduction; "2" little or little and ring finger unable to assume adduction; "3" little and ring finger unable to assume adduction or full extension; "4" little, right and middle unable to assume adduction or full extension.

Supplementary Table The scanning parameters of anatomic and diffusion MR image

Scanning mode	Imaging parameters
Sagittal T1W and T2W images	Field of view (FOV) = 250×250 mm, slice thickness = 3 mm, slice gap = 0.3 mm, fold-over direction = Feet/Head (FH), Number of excitation (NEX) = 2, resolution = $0.92\times1.16\times3.0$ mm^3 (T1W) and $0.78\times1.01\times3.0$ mm^3 (T2W), recon resolution = $0.49\times0.49\times3.0$ mm^3, Time of echo (TE) / Time of Repetition (TR) = 7.2 / 530 ms (T1W) and 120 / 3314 ms (T2W).
Axial T1W and T2W images	FOV = 80×80 mm, slice thickness = 7 mm, slice gap = 2.2 mm, fold-over direction = anterior/posterior (AP), NEX = 3, resolution = $0.63\times0.68\times7.0$ mm^3 (T1W) and $0.63\times0.67\times7.0$ mm^3 (T2W), recon resolution = $0.56\times0.55\times7.0$ mm^3 (T1W) and $0.63\times0.63\times7.0$ mm^3 (T2W), TE / TR = 8 / 1000 ms (T1W) and 120 / 4000 ms (T2W)
Axial diffusion tensor images	FOV = 80×80 mm, slice thickness = 7 mm, slice gap = 2.2 mm, fold-over direction = AP, NEX = 3, resolution = $1\times1.26\times7.0$ mm^3, recon resolution = $0.63\times0.64\times7.0$ mm^3, TE / TR = 60 ms / 5 heartbeats
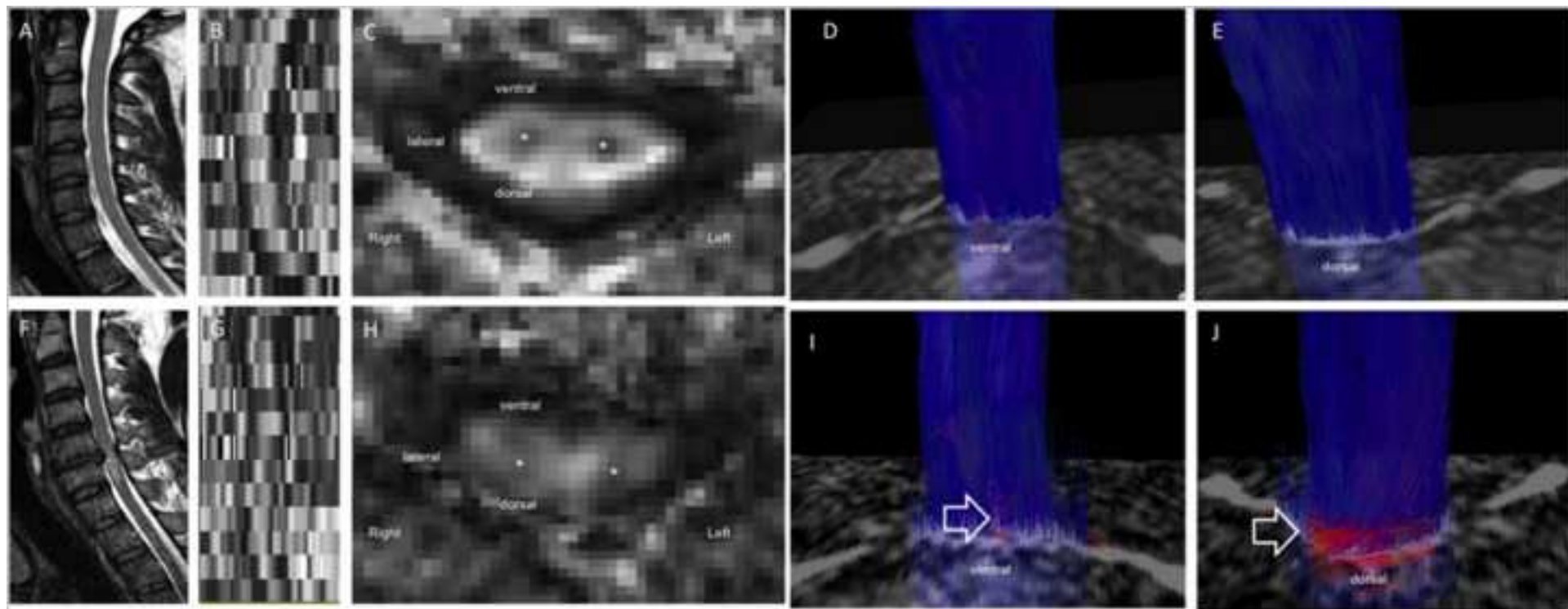
Figure2
Click here to download high resolution image

Figure3
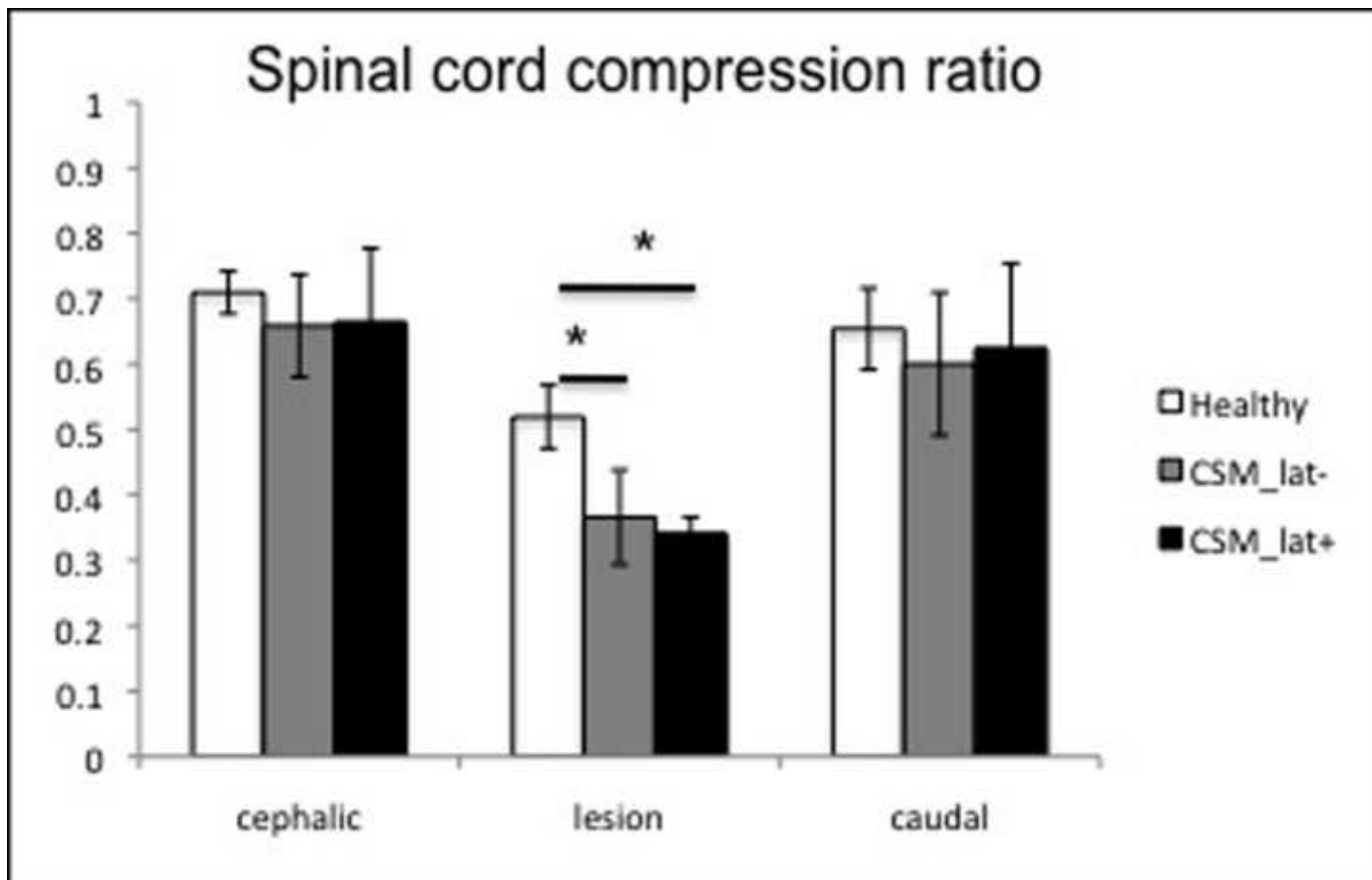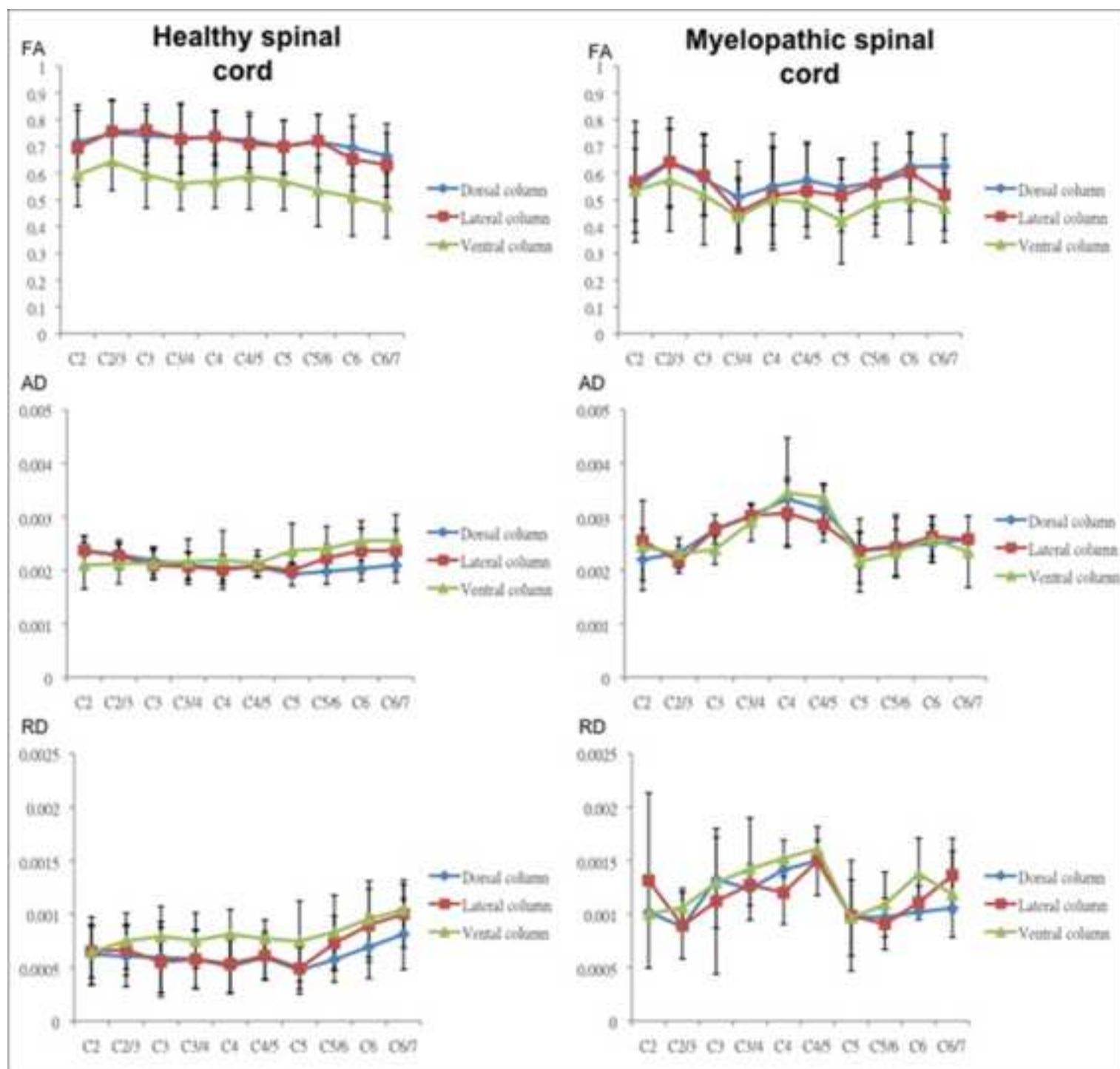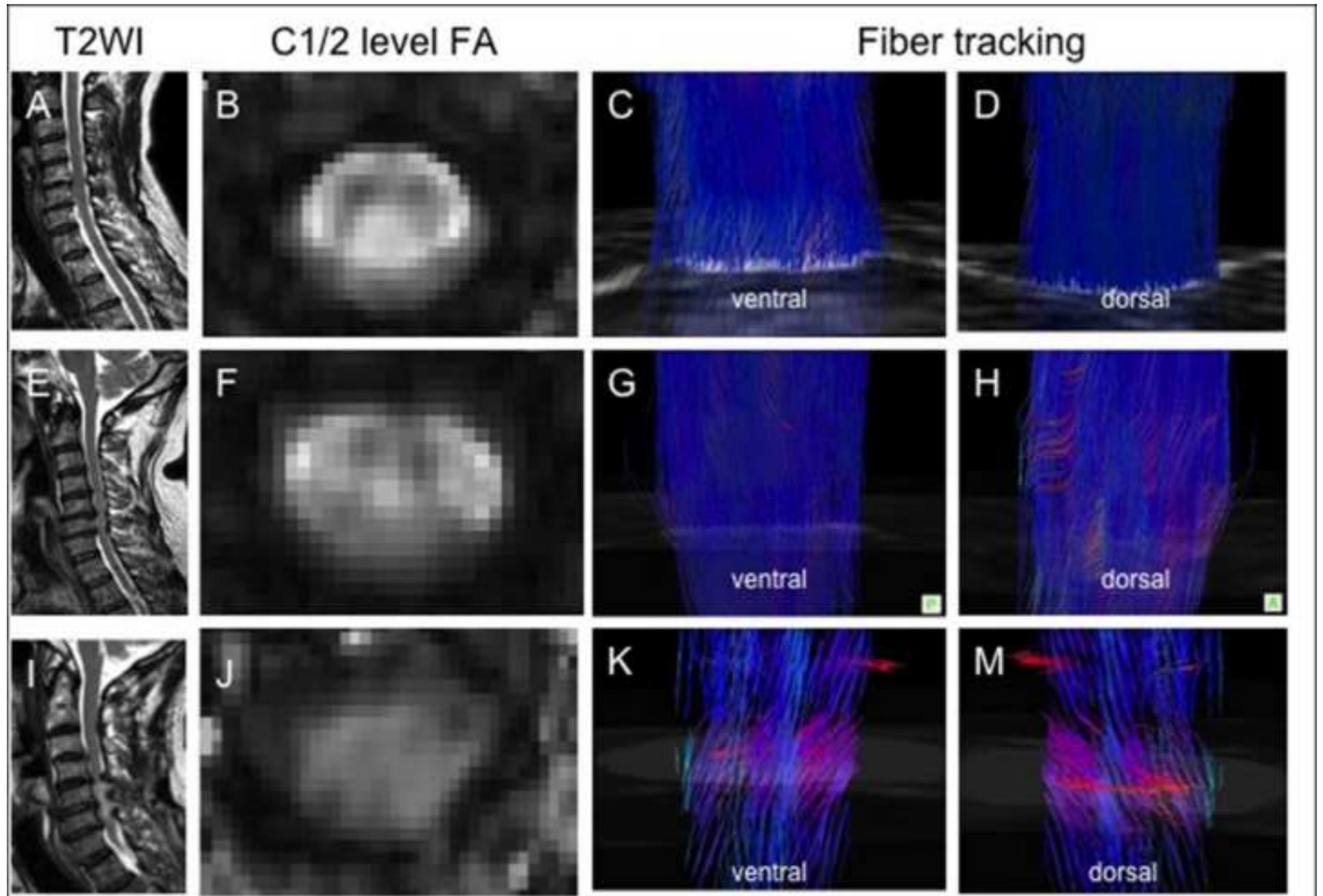**Click here to download high resolution image**

Figure 3

Figure4
Click here to download high resolution image

T2WI	C1/2 level FA	Fiber tracking	
A	B	C ventral	D dorsal
E	F	G ventral	H dorsal
I	J	K ventral	M dorsal

A: Fractional anisotropy of dorsal column B: Fractional anisotropy of lateral column C: Fractional anisotropy of Ventral column